IMPACT: International Journal of Research in Engineering & Technology (IMPACT: IJRET)
ISSN(E): 2321-8843; ISSN(P): 2347-4599
Vol. 3, Issue 4, Apr 2015, 47-56

MODELING OF RADON PROGENY DECAY IN RAINFALLS BASED ON GAMMA RAY MEASUREMENTS IN THE BRAZILIAN SECTOR

A. A. GUSEV[1], I. M. MARTIN[2] & M. A. ALVES[3]

[1]Space Research Institute of the Russian Academy of Sciences, Moscow, Russia

[2]Technological Institute of Aeronautics, ITA, São José dos Campos, SP, Brazil

[3]Institute of Aeronautics and Space, IAE/AMR, São José dos Campos, SP, Brazil

ABSTRACT

A method of a simulation of radiation fallout concomitant atmospheric liquid precipitations is proposed. The fallout is reconstructed from observed gammas through a numerical solution of the first kind Volterra integral equation describing variation of nuclide amount produced by precipitating ^{214}Pb and ^{214}Bi. Application of the method is considered on the examples of rainfalls in Brazil. There was an observed short fallout enhancement in the initial phases of the rains. It was demonstrated that nuclide quantity per unit of precipitated water decreases with increasing rainfall rate. The results obtained is compared with other observations and model.

KEYWORDS: Radiation Fallout, γ-Ray

INTRODUCTION

Radon and its progenies are natural radioactive nuclides found in the atmosphere all over the globe. Studies of the natural atmospheric radiation are of a great importance in applications as human health safety and radiation security of nuclear plants. Observation of various component of the natural and anthropogenic radiation is a helpful instrument in studies of atmospheric chemistry and physics of aerosols, cloud formation and rainfall of short and long period.

^{222}Rn and ^{220}Rn radon isotopes produced in decay chains of primordial ^{238}U and ^{232}Th contained in the earth's crust:

Basing on cosmological notions the ^{232}**Th**/^{238}**U** abundance ratio is estimated at 2 to 4. However, because of their half-life ratio,

$$\tau_{232Th}/\tau_{238U}=14.1\cdot 10^{9}\text{yr}/4.5\cdot 10^{9}\text{yr}=3.13$$

The production rate of radon isotopes should be quite close. The local ^{222}**Rn**/^{220}**Rn** production ratio depends on geological characteristics of the terrain, but in the near ground their concentrations are generally similar in order of magnitude.

After exulting from the earth, radon being an inert gas is able easily disperse into the atmosphere not adhering by itself to the precipitants. However ^{220}Rn with its relatively short half-life τ_{220Ra}=55 *sec* remains quite near to the ground providing noticeable ^{208}Tl gamma line in the decay chain:

$$^{220}\text{Rn}\xrightarrow{55\,\text{sec}}{}^{216}\text{Po}\xrightarrow{0.14\,\text{sec}}{}^{212}\text{Pb}\xrightarrow{10.6\,\text{hr}}{}^{212}\text{Bi}\xrightarrow{61\,\text{min}}{}^{208}\text{Tl}\xrightarrow{30\,\mu\text{sec}}{}^{210}\text{Pb}$$

(the values above the arrows indicate half-life of the corresponding radionuclide)

Opposite to that ^{222}Rn with its much longer half-life $\tau_{^{222}Ra}$**=3.8** day disperse into the whole atmosphere populating it with progenies from the decay chain:

$$^{222}Rn \xrightarrow{3.8\ day} {}^{218}Po \xrightarrow{3.1\ min} {}^{214}Pb \xrightarrow{26.8\ min} {}^{214}Bi \xrightarrow{20\ min} {}^{214}Po \xrightarrow{164\ \mu sec} {}^{210}P \qquad (2)$$

Owing to their longer half-life ^{214}**Pb** and ^{214}**Bi** are the most abundant radon progenies in the atmosphere. The solid radon progenies become airborne and immediately attach to the dust particles, aerosols and water droplets existing in the atmosphere. These particles undergo intensive convection aligning its concentration in the atmosphere (Kumar, et al., 1999). The droplets in clouds aggregate into raindrop and precipitate to the ground surface. The concentration of adsorbed/absorbed radionuclides in raindrops determine specific radionuclide fallout characterized by radioactivity per unit of liquid precipitations.

In spite of the fact that basic physics of cloud formation and precipitation is known (Nobuyoshi and Katase, 1984) no comprehensive quantitative model of the phenomenon has still been developed, due to the insufficient accuracy of our knowledge of parameters of the processes in clouds. Taking this point of view, the observation of the fallout dynamics may be a helpful instrument for verification of current models and adjusting their parameters. The half-lives of ^{214}**Pb** and ^{214}**Bi** are on the same scale as precipitation events, and thus are suitable for monitoring.

Radiochemical methods and solid state track detectors allowing direct detection of radionuclides are rather complicated that hampers their usage for continues long-term observations. Opposite to that measurements of the γ-emission produced by fallout can be performed with relatively simple scintillation (e.g. Paatero and Hatakka, 1999) and solid-state detectors (e.g. Ichiji and Hattori, 2000). Nishikawa et al., (1989) confirmed through numerical simulation that during a rainfall a crystal or solid-state detector registers at the ground level gammas emitted from the encircling surface. This area increases with the energy of γ-quanta from 80 *m* for 0.2 *MeV* to 200 m for 3 *MeV*. A certain difficulty of these measurements is a rather low fallout intensity in comparison with the background. Due to that, the measurements require large detector volumes and/or accumulation of the rainfall water to increase concentration of precipitated radionuclide in the immediate vicinity of the gamma detector. It is especially important if it is measured not rough gamma intensity only but its energy distribution.

Using this experimental approach Hornga and Jianga (2004) evaluated duration of a stage in which cloud droplet collide with each other forming raindrops, Greenfield, et al, (2008) estimated the time raindrops need to reach a ground from a cloud. He also (Greenfield, et al, 2003) explored a possibility of monitoring rainfall rate through γ-ray observation. In all this studies rainfall data with time resolution less than a quarter of an hour were used.

Monitoring of radon progenies is of special interest in Brazil because it is likely a place with the highest level of primordial radioactivity on the globe. City of Sao Jose dos Campos is one of the most important industrial and research centers in Latin America with emphasis in aerospace science and technology. A laboratory of environmental radiation of Centro Técnico Aeroespacial (Sao Jose dos Campos, SP, Brazil, 23°11′11″ S, 45° 52′ 43″ W, 650 *m* altitude) performs a continuous monitoring of near ground radiation of natural and anthropogenic origin both with the aim of pollution control and for studies in the area of atmospheric physics. The station facilities allow registration of both neutral (gammas, neutrons and charged particles). They include several scintillation detectors of various volumes, gas-discharge detectors

and α-particles detectors. This paper presents recent results of observation of radiation dynamics related with rainfalls.

METHOD AND EXPERIMENT

Fallout ***F* (*t*)** in a moment *t* results in a radionuclide density ***N*(*T*)** in a subsequent moment *T* :

$$N_{214Pb}(T) = F_{214Pb}(t)e^{-\frac{T-t}{t_{214Pb}}} \quad \text{(a)}$$

$$N_{214Bi}(T) = F_{214Bi}(t)e^{-\frac{T-t}{t_{214Bi}}} + F_{214Pb}(t)t_{214Bi}\frac{e^{-\frac{T-t}{t_{214Pb}}} - e^{-\frac{T-t}{t_{214Bi}}}}{t_{214Pb} - t_{214Bi}} \quad \text{(b)} \qquad (3)$$

The total radionuclide density is $N(T) = N_{214Pb}(T) + N_{214Bi}(T)$.

The ^{214}**Po** isotope is not included to the system because it practically instantaneously (τ_{214Po}=164 μ*sec*) decays to the stable ^{210}Pb and its input to the total density is negligible.

The instantaneous γ-intensity $G(T)$ is $G(T) = N_{214Pb}(T)/\tau_{214Po} + 2N_{214Bi}(T)/\tau_{214Bi}$ (4)

A factor 2 at N_{214Bi} density accounts for the ^{214}Po decay.

In the absence of a direct ^{214}Bi fallout ($F_{214Bi}(t)$=0) and (T-t)→∞ the solution of Eq.3 represents so called transient equilibrium with the ratio $N_{214Pb}(t)/N_{214Bi}(t) = \varepsilon_d = \tau_{214Bi}/(\tau_{214Pb} - \tau_{214Bi})$=2.74. If the fallout $F_{214Pb}(t)$=const i.e. does not depend on time, $F_{214Bi}(t)$=0 and $T\to\infty$ than the ratio $N_{214Bi}(t)/N_{214Pb}(t) = \varepsilon_e = \tau_{214Bi}/\tau_{214Pb}$ =0.74 describes a so called secular equilibrium, when the rates of change of the isotopes in a decay chain are equal and their concentrations are unchanging. The corresponding ratio of γ-ray rates is $G_{214Bi}(t)/G_{214Pb}(t)$ =1. In the real atmosphere the N_{214Bi}/N_{214Pb} ratio may differ from ε_e (see for example Forkapić, et al., 2013)

Integration of Eq.3 over *t* results to:

$$G(T) = \int_0^T \left[\frac{1}{t_{214Pb}}F_{214Pb}(t)e^{-\frac{T-t}{t_{214Pb}}} + \frac{2}{t_{214Bi}}F_{214Bi}(t)e^{-\frac{T-t}{t_{214Bi}}} + 2F_{214Pb}(t)\frac{t_{214Pb}}{t_{214Bi}}\frac{e^{-\frac{T-t}{t_{214Pb}}} - e^{-\frac{T-t}{t_{214Bi}}}}{t_{214Pb} - t_{214Bi}}\right]dt \qquad (4)$$

When the ratio $F_{214Bi}(t)/F_{214Pb}(t)=\varepsilon_c$ is known/assumed and does not depend on time, Eq.3 transforms to a classic linear first kind Volterra integral equation with a difference kernel $K(T-t)$ (Polyanin and Manzhirov, 2008):

$$G(T) = \int_0^T F(t)K(T-t)dt \qquad (5)$$

In our case an unknown function $F(t) = \varepsilon F_{214Pb}(t)$ and

$$K(T-t) = \frac{1}{t_{214Pb}}e^{-\frac{T-t}{t_{214Pb}}} + \frac{2e}{t_{214Bi}}e^{-\frac{T-t}{t_{214Bi}}} + 2\frac{t_{214Pb}}{t_{214Bi}}\frac{e^{-\frac{T-t}{t_{214Pb}}} - e^{-\frac{T-t}{t_{214Bi}}}}{t_{214Pb} - t_{214Bi}}$$

Eq.5 has a unique solution and $F(t)$ can be simulated numerically through the following step by step procedure:

$$F(ih) = \frac{1}{K(0)}\left\{2\left[\frac{G(ih) - G((i-1)h)}{h} - \sum_{j=1}^{i-1} F(jh)\left[K((i-j+1)h) - K((i-j)h)\right]\right] - K(h)\right\}, \quad (6)$$

here a known function $G(T)$ is given in a table form with a step h, $T=ih$, $t=jh$

RESULTS

The gamma total γ-ray flux and spectrum are measured in the 0.03-10 MeV energy range using two 3"×3" NaI(Tl) detectors with maximum sampling frequency 1 min.

A measured gamma spectrum in Figure 1 demonstrates a presence of ^{222}Ra progenies: ^{214}Pb (0.295 *MeV* peak), ^{214}Bi (0.609, 1.052 *MeV* peaks) and that of ^{220}Rn: ^{208}Tl (2.6*MeV* peak). The strongest 1.46 line is produced by primordial ^{40}K radionuclide.

Figure 2 presents an example of a γ-rate record for a March 19 – April 23 2012 in the end of a rainy season characterized with a quite low level of liquid precipitation. Clear diurnal oscillation of the γ-ray intensity of about 5% is controlled by small scale eddy dynamics of the low atmospheric boundary layer due to variations of the temperature and humidity of the atmosphere and soil.

One can see that all the variations with amplitude exceeding ≈520 *Bq/sec* are accompanied with rains or fogs (the latter also can be considered as some type of precipitation). During the rainfalls γ-ray intensity increases up to 15%.

Several events of these events are depicted in Fig.3 in an enlarged scale. The shortest leading edge of observed γ-ray enhancements is about 10 minutes. Thus corresponding variations of the fallout and rainfall rate are of the same or shorter time. Due to that, routine precipitation data of 1 hour or lower resolution provided by meteorological stations are not adequate for such studies. To provide necessary data a set of instruments for simultaneous observation of the natural gamma background and meteorological parameters with time up to 1 minute was installed and come into operation in the 2012 (Martin et al., 2014).

Figure 3 also includes reconstructed fallouts for the considered events. Noteworthy variety of profiles, due to differences in parameters and mechanisms caused precipitations. It is very clearly seen in the events of March 3 and 27 2012 that the leading edge of the gamma enhancement is controlled by fallout rate and the trailing edge after rain termination is determined purely by decay constants.

Figure 4a demonstrates a γ-rate record, simulated fallout, specific fallout and rainfall rate for a sequence of two prolonged rains in Jul 23 - 25 2013 (South America dry season): rain **A** lasted from 30 to 55 hour, rain **B** from 61 to 83. The integral characteristics of the events of the rains are listed in Table 1. A dotted curve demonstrates a result of the inverse simulation i.e. that of the observed γ-rate from the simulated fallout through Eq.4.

Comparison of the panels **a** and **b** in Figure 4 demonstrates that the simulated fallout is proportional in the main to the rainfall rate. In the same time, the relation between the specific fallout and rainfall rates is inverse. It is especially well seen for the fallout peaks (marked with 1, 2, 3, 4, 5 in the panel **a**) all corresponding to low rainfall rate. In the same time several rainfall peaks located between hours 73 and 80 are not accompanied with those of specific fallout. The rest of the

rainfall these parameters slightly oscillate near a mean values against significant variation of the rainfall rate especially in the second rain **B**. One can also see from the Table 1 that at close mean of γ-rate and total fallout values of the two rains the corresponding rainfall parameters differs by about one order.

Table 1: Characteristics of the Rainfalls Jul 23 - 25 2013

	Units	Rain A	Rain B
Location on timescale of Figure 7, 8	*min*	1800 – –3600	3600 – – 5000
Duration	*hr*	25	22
Precipitation level	*mm*	8	60
Mean rainfall	*mm/hr*	0.32	3
Maximal rainfall rate	*mm/hr*	2	30
Mean raindrop diameter*	*mm*	0.7	0.8
Total fallout	*Bq*	50	60
Mean γ-rate	*Bq/min*	2	3
Maximal of γ-rate enhancement	*Bq/min*	4000	8000
Mean specific fallout	*Bq/mm*	5.1	0.9

*The mean raindrop diameter $\overline{d}$ is calculated from the Marshall –Palmer (1948) empirical relationship $N_{rd}(d)=8000 \exp(R^{-0.21}d)$, where d is a raindrop diameter and R is f rain rate in *mm /h* confirmed by later measurements (Peters et al., 2002) of Doppler shift .

The effect of the inverse dependence between the specific fallout and the rainfall is illustrated by Figure 5 where a dependence of the total accumulated fallout versus the total accumulated rainwater is depicted. Thus the slope of the curve segment is determined by specific fallout rate. A “knee” in the curve at about 8 *mm* on the accumulated rainfall axis coincides with the beginning of the rain **B** at 3800 *min* at time scale of Fig.4b. For the rain **A** the inclination is 5.1 and for the rain **B** 0.9 1*/mm*.

DISCUSSIONS

One can see from the Fig. 5 that in spite of the sharp peaks of a few minutes width, on a larger scale of ≈1 *hour* the γ-rate is linearly proportional to the rainfall rate. A proportionality factor differs in different rains but does not practically change within same rain that means a specific fallout constancy. The latter feature was also observed by Fujinami (2003). However it does not quite agree with a work of Greenfield at al. (2003) where γ-rate in same rain is proportional to the (rainfall rate)$^{0.45}$ i.e. specific fallout is proportional to (rainfall rate)$^{-0.55}$. The inverse relation between a rainfall rate and a specific fallout was also observe by Fujinami (2003) and Paatero and Hatakka, (1999).

In the same time the integral characteristics of the two rains considered here quite agree with observation of cited authors. The relation obtained by Greenfield at al. (2003) being applied to specific rainfall ratio between separate **B** and **A** rains results in a value of 0.3, which is quite close to the observed one of 0.22. The inverse relation between rainfall and specific fallout was simulated in a numerical model of Minato (2007): according to it the ratio of specific fallouts for rainfall rates 3 and .32 mm/hr is ≈0.25 that is also quite close to the value measured in the present work.

Seems high γ-rate peaks in Figure 4 cannot be interpreted the same way as those for the large scales. Probably the effect is not related with precipitations but rather with short rising damps, analogues to that in March 3 2013 in Figure 3.

CONCLUSIONS

Radiation fallout was reconstructed from γ-ray observation using a numerical simulation of the first kind Voltera integral equation with difference kernel. The equation describes variation of nuclide amount produced in the decay chain of precipitating **^{214}Pb** and **^{214}Bi**. The difference kernel is determined by ratio of precipitating amounts of **^{214}Pb** and ^{214}Bi and their decay half times.

Application of the method is considered on example of rainfalls in Brazil. Sharp peaks of γ-radiations coinciding with initial moments of radiation raise were observed. The parameters of the observed inverse relation between γ-rate and rainfall well agree with results of other observations and simulations.

REFERENCES

1. Forkapić, S., Mrđa, D., Vesković, M., Todorović, N., Bikit, K., Nikolov, J., Hansmant, J. *Equilibrium Measurement in the Air*. Rom. Journ. Phys. **58**, S140–S147 (2013)
2. Fujinami, N. *Study of Radon Progeny Distribution and Radiation Dose Rate in the Atmosphere*, Jpn. J. Health Phys., **44**, 89-94 (2009)
3. Greenfield, M., Greenfield, A., Domondon, T., Tsuchiya, S., and Tomiyama, M., *Monitoring precipitation rates using γ-rays from adsorbed radon progeny as tracers.* Jap. J. Ap. Phys. **93**, 5733-5741 (2003)
4. Greenfield, M., Ito, A., Iwata, K., Ishigaki, M., Komura, K., *Determination of rain age via rays from accreted radon progeny*. J. Ap. Phys. **104**, 074912 (2008)
5. Hornga, M. and Jianga, S. *In situ measurements of gamma-ray intensity from radon progeny in rainwater*, Rad Meas. **38**, 23-30 (2004)
6. Ichiji, T., and Hattori, T., Continuous Measurement of Environmental Gamma Radiationin in Tokyo Using Ge Semiconductor Detector. http://www.irpa.net/irpa10/cdrom/00611.pdf (2000)
7. Kumar, A. V, Sitaraman, V., Oza, R. B., Krishnamoorthy T.M. *Application of a numerical model for the planetary boundary layer to the vertical distribution of radon and its daughter products*. Atm. Envir. **33**, 4717-4726 (1999)
8. Martin I. M., Gomes, P., A. Alves, Gusev, A., Pugacheva, G., *Monitoring of natural background gamma radiation at ground level in São José Dos Campos*, SP, Brazil, Int. J. Env. Ecol. Family Urb. Stud. **4**, (2014)
9. Marshall, J. S. and Palmer W. M. *The distribution of the raindrops with size*. J. Meteorol. **5**, 165-166 (1948)
10. Minato, S. *A Simple Rainout Model for Radon Daughters. J. Nuc. Radiochem. Sci*. **8**, p/N1-N3 (2007)
11. Nishikawa, S. Okabe and M. Aoki, Monte Carlo Calculation of Gamma-Ray Flux Density Due to Atmospheric Radon Daughters, J. Nucl. Sci. Technol., **26**, 525-529 (1989)
12. Nobuyoshi, T. and Katase, A., Rainout-Washout Model for Variation of Environmental Gamma-Ray Intensity by Precipitation, J. Nucl. Sci. Tech., **19**, 393-409 (1982)
13. Paatero. J. and Hatakka, J. Paatero & Hatakka Wet deposition efficiency of short-livedradon-222 progeny in

central Finland, Boreal Env. Res **4**, 285–293 (1999)

14. Peters, O., Hertlein, C. and Christensen, K. A Complexity View of Rainfal. Phys. Rev. Lett. 88, 01870, (2001)
15. D. Polyanin and A. V. Manzhirov, Handbook of Integral Equations, 2nd Edition, Chapman & Hall/CRC, 2008

APPENDICES

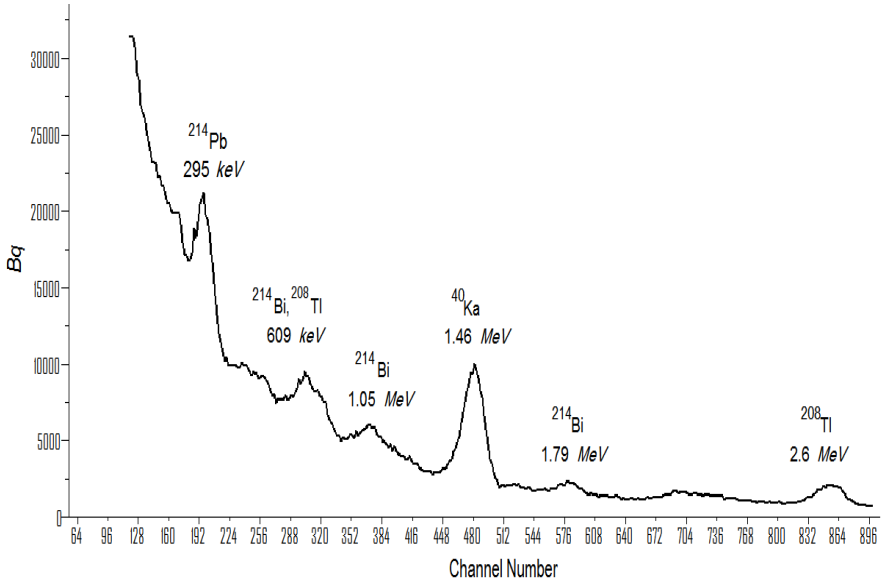

Figure 1: A Gamma Spectrum Measured with 3"×3" Nai(Tl) Scintillation Detector

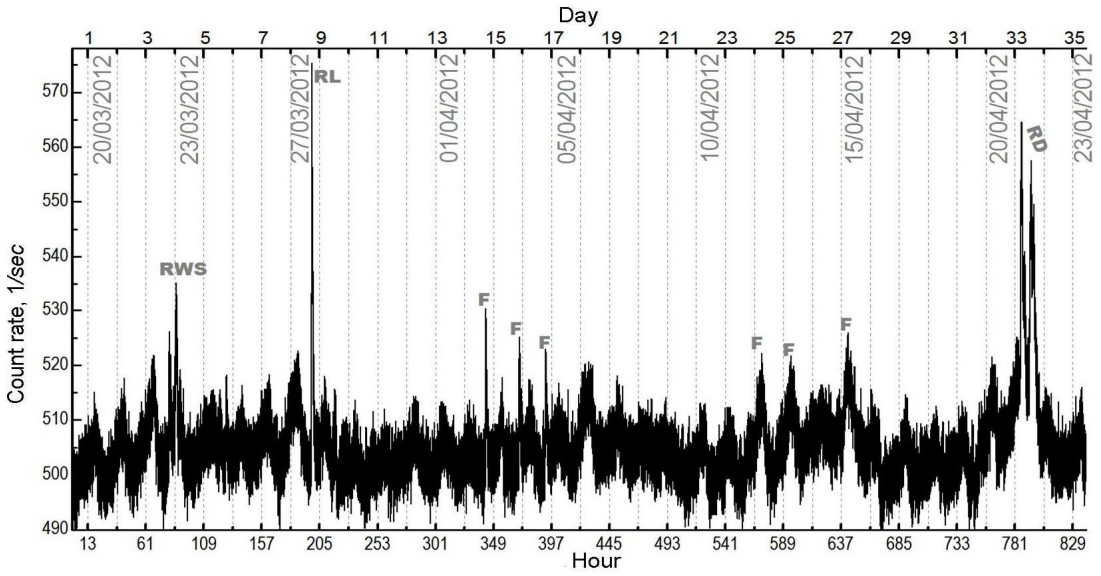

Figure2: Time History of the γ-Ray Detector. Abbreviations in Grey Bold Marks Events of Precipitation: F – Fog, RWS – Weak Short Rain, SL – Shower with Lightning, RD – Lasting Drizzling Rain. Permanent Background Component of 40000 1/Sec Is Subtracted

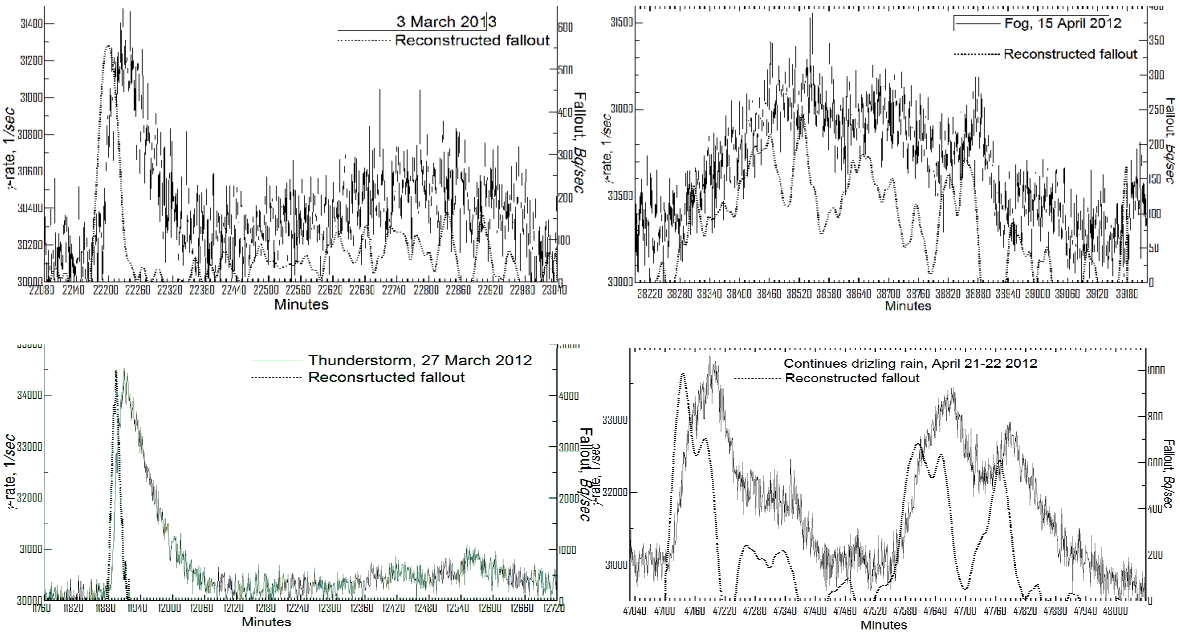

Figure 3: Examples of Simulated Fallouts for the Precipitation Events from Figure 2

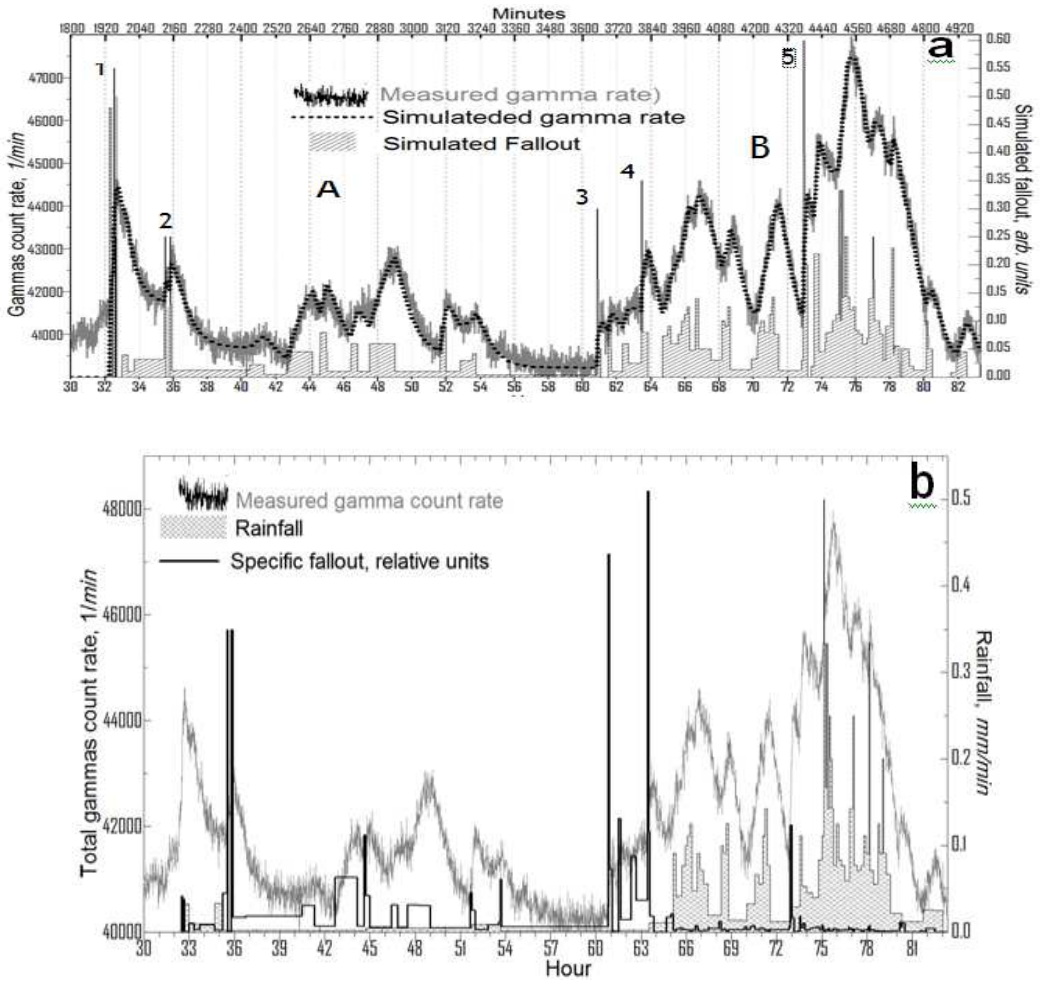

Figure 4: Comparison of the Measured $\gamma$and Rainfall Rates with Simulated Fallout a nd Specific Fallout

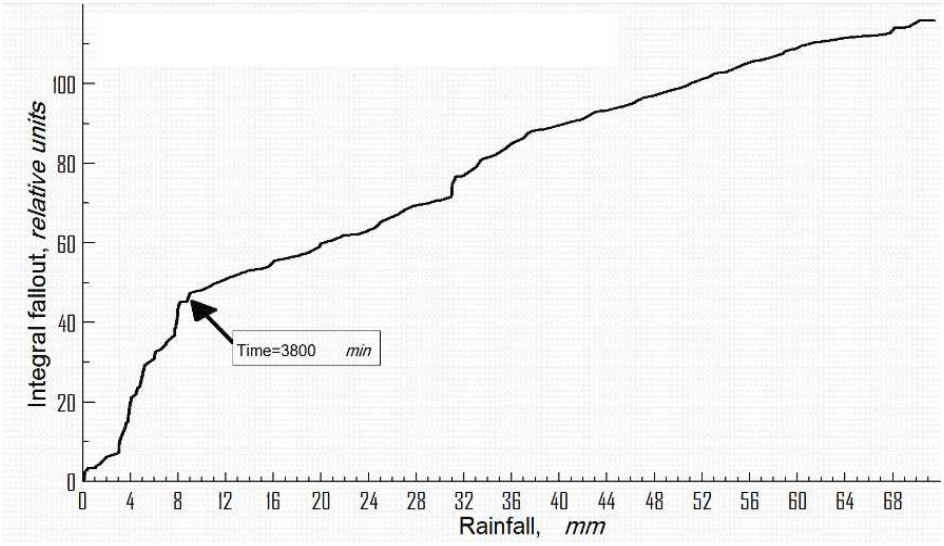

Figure 5: Dependence of the Total Accumulated Fallout on the Total Rainfall Level for the Rainfall Shown in Figure 4